Observation of Vector Vortex Lattices in Polarization States of an Isotropic Microcavity Laser

Y. F. Chen,* K. F. Huang, and H. C. Lai

Department of Electrophysics, National Chiao Tung University, Hsinchu, Taiwan, Republic of China

Y. P. Lan

Institute of Electro-Optical Engineering, National Chiao Tung University, Hsinchu, Taiwan, Republic of China

We experimentally investigate the formation of a vector polarization pattern from an isotropic microcavity laser. It is found that the orthogonal components of the observed pattern are localized on the geometrical rays. The connection between eigenfunctions and geometrical rays is analytically constructed by using the SU(2) coherent states. With the analytical function form, the observed vector pattern is completely reconstructed and the vector vortex lattice is apparent.

Vortices appear in various aspects of modern physics such as vortex lattices in superconductors, quantum Hall effects, and Bose-Einstein gases [1–3]. In a light wave, the phase singularity of the complex scalar field forms an optical vortex [4–6]. Both single optical vortex and optical vortex lattices have been experimentally observed in lasers [7,8]. In addition to scalar vortices, paraxial optical fields can exhibit vector vortices associated with a space-dependent polarization [9–11]. The single vector vortex has been experimentally observed in CO_2 lasers [12] and in vertical cavity surface emitting lasers (VCSELs) [13]. However, the vector vortex lattice thus far has not been observed in lasers. The difficulty of forming a vector vortex lattice is that the laser cavity needs to be a large Fresnel number and high-level isotropic.

Recently, Hegarty *et al.* [14] reported interesting transverse mode patterns from oxide-confined square shaped VCSELs with large Fresnel number. Their experimental results reveal that a wave incident upon the oxide boundary would undergo total internal reflection because of large index discontinuities between the oxide layer and the surrounding semiconductor material. In this work, we present an experimental observation of vector vortex lattices in a square shaped VCSEL with large aperture. Experimental results reveal that the transverse mode of the square shaped VCSEL can display a vector polarization pattern associated with the geometrical ray when the thermal effects and the cavity anisotropies are reduced. To explain the observed pattern, we use the SU(2) coherent states to analytically connect the eigenfunctions with the geometrical rays. With the SU(2) coherent state, the observe vector pattern is completely reconstructed and the vector vortex lattice is manifest.

In this investigation, we fabricate square shaped VCSELs with large aperture and measure near-field transverse patterns. The size of the oxide aperture is 40×40 μm^2. The device structure of these oxide-confined VCSELs is similar to that described by Ref. [14]. The effective cavity length between two distributed feedback reflectors is designed to have the emission wavelength around $\lambda_z = 799.5$ nm. The near-field patterns are measured with a CCD camera (Coherent, Beam-Code) and an optical setup similar to that described in Ref. [14]. An optical spectrum analyzer (ADVANTEST Q8347) is used to monitor the spectral information of the laser.

The performance of the VCSEL device is measured at a temperature around $0\,°C$. It is found that near lasing threshold the transverse pattern is linearly polarized, but the polarization is not the same for different points of the transverse plane. In other words, the observed pattern is a vector pattern formation and its polarization is position dependent. The measurement of the optical spectrum verifies that the observed transverse pattern is phase synchronized to a single frequency at 795 nm. Even though a single-frequency high-order transverse pattern has been observed in VCSELs [14], it is usually a scalar pattern formation; i.e., the polarization is always the same for all points of the transverse plane. The basic requirement for a vector polarization pattern is that the orthogonal polarization modes with different spatial patterns are phase synchronized to a common frequency. The polarization modes normally are frequency degenerate; however, strain or electric field induced birefringence may lift the degeneracy to the order of $\Delta\lambda = 0.05$ nm [15]. We find that about half the present fabricated devices can have the property of the frequency locking between the polarization modes. Therefore, we speculate that the frequency locking between the polarization modes is subject to the degree of birefringence effect. Figures 1(a) and 1(b) show the polarization resolved near-field patterns in the $45°$ and $-45°$ direction, respectively. The polarization angle is referring to the [110] direction of the (001)-GaAs crystal. It can be seen that near-field components of orthogonal polarizations have different pattern structures. Since the orthogonally polarized near-field patterns are phase synchronized to a common frequency, the orthogonally polarized components can mutually interfere to lead to a greatly different pattern in the polarization resolved near-field image, as shown in Fig. 1(c) for $0°$ polarization.
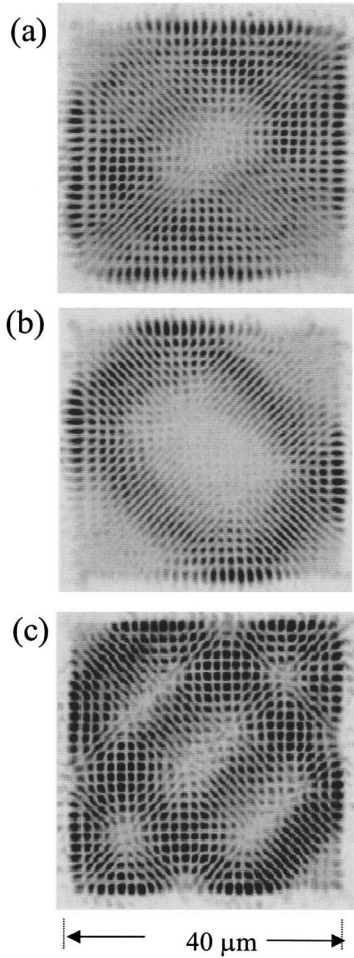
FIG. 1. Experimental polarization resolved pattern emitted from the VCSEL device near lasing threshold: (a) $-45°$ polarization; (b) $+45°$ polarization; (c) $0°$ polarization.

In order to understand the observed transverse patterns, we consider the large aperture VCSEL to be a planar waveguide with a dominant wave vector along the vertical direction. According to the waveguide theory [16], the electromagnetic fields with a predominant z direction of propagation can be approximated as $\vec{E}(x, y, z, t) = \vec{E}(x, y)e^{i(\beta z - \omega t)}$, where ω is the angular frequency and β is the propagation constant along the z direction. After separating the z dependence in Maxwell equation, we are left with a two-dimensional (2D) Helmholtz equation: $(\nabla_t^2 + k_t^2)\vec{E}(x, y) = 0$, where $k_t^2 = (\omega/c)^2 - \beta^2$, and c is the wave speed. Since the photons will experience total reflection at the lateral oxide walls, the extension of the evanescent field is reduced. Therefore, we approximate the wave function to obey the condition of $\vec{E}(x, y) = 0$ on the boundary.

As is well known, the eigenfunction for the Helmholtz equation with a square rigid boundary is given by

$$\psi_{m,n}(x, y) = \frac{2}{a}\sin\left(\frac{m\pi x}{a}\right)\sin\left(\frac{n\pi y}{a}\right), \tag{1}$$

$$k_t^2 = \left(\frac{m\pi}{a}\right)^2 + \left(\frac{n\pi}{a}\right)^2. \tag{2}$$

Since the functional form of the present resonator is similar to the 2D Helmholtz equation, it is possible to describe $\vec{E}(x, y)$ with the eigenfunctions $\psi_{m,n}(x, y)$. However, the subtle solution in Eq. (1) cannot account for the present observed pattern localized on the geometrical trajectories. Recently, Pollet *et al.* [17] demonstrated that the wave function of the SU(2) coherent state for the 2D quantum harmonic oscillation is well localized on the corresponding classical elliptical trajectory. As in the Schwinger representation of the SU(2) algebra [18], SU(2) transverse mode functions for a square planar waveguide are expressed as [19]

$$\Psi_N(x, y; \phi) = \left(\frac{2}{a}\right)\frac{1}{2^{N/2}}\sum_{K=0}^{N}\binom{N}{K}^{1/2}e^{iK\phi}\sin\left[(K+1)\frac{\pi x}{a}\right]$$
$$\times \sin\left[(N-K+1)\frac{\pi y}{a}\right], \tag{3}$$

where the parameter ϕ is related to the wall positions of specular reflection points and the quantity $\binom{N}{K}$, which equals $N!/[K!(N-K)!]$ is a binomial coefficient. The index N is related to the average value of $\langle k_t^2 \rangle$. Experimentally, the value of N is determined by the detuning between the longitudinal cavity resonance and the gain emission frequency. The relationship between the parameter ϕ and the periodic orbits can be understood by using the identity of $\sin z = (e^{iz} - e^{-iz})/2i$ to rewrite Eq. (3) and applying the property of the *Dirichlet kernel*. Numerical calculations show that the behavior of $|\Psi_N(x, y; \phi)|^2$ agrees very well with the geometrical trajectory (classical periodic orbit), as shown in Fig. 2. To our knowledge, it is original to use the eigenfunctions of the Helmholtz equation with a square rigid boundary to describe the VCSEL transverse modes.

The wave function given in Eq. (3) represents a traveling-wave property. The standing-wave representations can be obtained by using $\Psi_N(x, y; \phi) \pm \Psi_N^*(x, y; \phi)$. Although the wave function representation in Eq. (3) consists of $N + 1$ eigenstates, numerical analyses reveal that a superposition of only a few eigenstates is already sufficient to result in the localization on the classical trajectory. To include this property, the partially coherent states for the standing wave can be expressed as

$$\Psi_{N,M}^c(x, y; \phi) = \frac{(2/a)}{\left[\sum_{K=q}^{N-q}\binom{N}{K}\cos^2 K\phi\right]^{1/2}}\sum_{K=q}^{N-q}\binom{N}{K}^{1/2}(\sin K\phi)\sin\left[(K+1)\frac{\pi x}{a}\right]\sin\left[(N-K+1)\frac{\pi y}{a}\right], \tag{4}$$

and

$$\Psi^s_{N,M}(x,y;\phi) = \frac{(2/a)}{\left[\sum_{K=q}^{N-q}\binom{N}{K}\cos^2 K\phi\right]^{1/2}} \sum_{K=q}^{N-q}\binom{N}{K}^{1/2}(\sin K\phi)\sin\left[(K+1)\frac{\pi x}{a}\right]\sin\left[(N-K+1)\frac{\pi y}{a}\right] \tag{5}$$

where the index $M = N - 2q + 1$ represents the number of eigenstates used in the wave function. Using Eqs. (4) and (5) to fit the experimental result, it is found that $E_-(x,y) = \Psi^s_{53,4}(x,y;-0.38\pi)$ and $E_+(x,y) = \Psi^c_{53,8}(x,y;0.59\pi)$, where $E_-(x,y)$ and $E_+(x,y)$ are the field distribution for the observed patterns in the $-45°$ and $+45°$ direction, respectively. In terms of $E_-(x,y)$ and $E_+(x,y)$, the field distribution for the observed pattern can be expressed as

$$\vec{E}(x,y) = E_x(x,y)\vec{a}_x + E_y(x,y)\vec{a}_y, \tag{6}$$

where

$$E_x(x,y) = [\Psi^c_{53,8}(x,y;0.59\pi) + \Psi^s_{53,4}(x,y;-0.38\pi)]/\sqrt{2}, \tag{7}$$

and

$$E_y(x,y) = [\Psi^c_{53,8}(x,y;0.59\pi) - \Psi^s_{53,4}(x,y;-0.38\pi)]/\sqrt{2}. \tag{8}$$

The polarization resolved near-field patterns shown in Fig. 1 are numerically reconstructed by $|E_-(x,y)|^2$, $|E_+(x,y)|^2$, and $|E_x(x,y)|^2$, as depicted in Fig. 3. The excellent agreement between the experimental and recon-

structed patterns evidences that the oxide-confined VCSEL cavity can be considered as a planar waveguide. Moreover, it is greatly important to note that the eigenstates used to expand the observed transverse patterns are not exactly degenerate but nearly degenerate. This result indicates that the spontaneous transverse mode locking within almost-degenerated modes plays an important mechanism in the laser pattern formation [20]. Another intriguing point is that the observed patterns of Fig. 2(b) are similar to the diamond-shape scar that has been discussed extensively in the wave functions of ballistic quantum dots [21,22].

With the analytical function given in Eqs. (6)–(8), the polarization pattern of the observed mode is illustrated in Figs. 4(a) and 4(b) for global view and zoom-in view, respectively. The vector vortex lattice can be clearly seen from the zoom-in view. To our knowledge, the preset
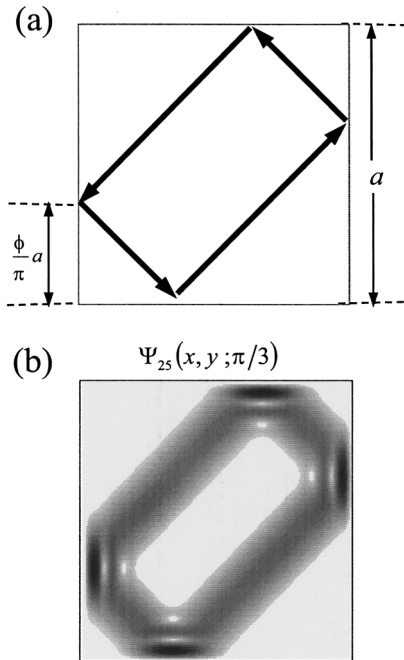

FIG. 2. (a) A typical ray trajectory. (b) The wave pattern $|\Psi_N(x,y;\phi)|^2$ from Eq. (3) for $N = 25$.
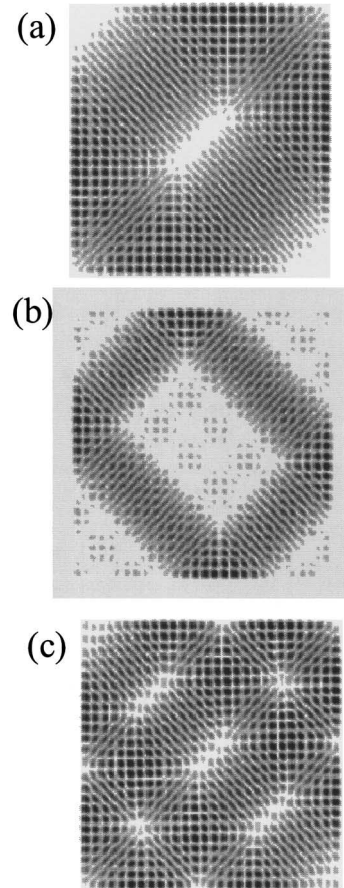

FIG. 3. Theoretically reconstructed patterns for the results shown in Fig. 1, calculation with Eqs. (6)–(8).
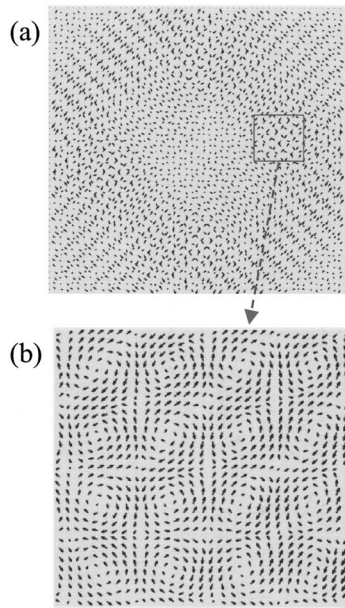
FIG. 4.   Numerically calculated polarization planes for the observed pattern (a) global view; (b) zoom-in view.

experiment provides the first observation of a vector vortex lattice in an isotropic laser. Although the mode order may change with changing the temperature, the basic pattern formation does not change. Moreover, the observed pattern retains its identity even when the pump current increases about $1 \sim 3$ mA. In other words, the observed pattern is generic and structurally stable.

In summary, a vector polarization pattern has been observed in an isotropic microcavity laser. The observed transverse patterns are analytically reconstructed by using the partially coherent states. With the analytical function, the formation of vector vortex lattices in the observed pattern is clearly shown.

*Author to whom correspondence should be addressed.
Permanent address: Department of Electrophysics, National Chiao Tung University, 1001 TA Hsueh Road, Hsinchu, Taiwan, 30050.
Electronic address: yfchen@cc.nctu.edu.tw

[1] G. Blatter, M. V. Feigelman, and V. B. Geshkenbein, Rev. Mod. Phys. **66**, 1125 (1994).
[2] R. E. Prange and M. Girvin, *The Quantum Hall Effect* (Springer-Verlag, Berlin, 1990), 2nd ed.
[3] F. Dalfovo, S. Giorgin, L. P. Pitaevskii, and S. Stringari, Rev. Mod. Phys. **71**, 463 (1999).
[4] J. F. Nye and M. V. Berry, Proc. R. Soc. London A **336**, 165 (1974).
[5] M. V. Berry, *Physics of Defects*, Proceedings of the Les Houches Summer School, Session XXXV (North-Holland, Amsterdam, 1981), p. 453.
[6] M. V. Berry, Proc. SPIE **3487**, 1 (1998).
[7] C. Tamm, Phys. Rev. A **38**, 3960 (1988).
[8] Y. F. Chen and Y. P. Lan, Phys. Rev. A **64**, 063807 (2001).
[9] L. Gil, Phys. Rev. Lett. **70**, 162 (1992).
[10] L. M. Pismen, Physica (Amsterdam) **73D**, 244 (1994).
[11] J. F. Nye and J. V. Hajnal, Proc. R. Soc. London A **409**, 21 (1987).
[12] C. Taggiasco, R. Meucci, M. Ciofini, and N. B. Abraham, Opt. Commun. **133**, 507 (1997).
[13] F. Prati, G. Tissoni, M. S. Miguel, and N. B. Abraham, Opt. Commun. **143**, 133 (1997).
[14] S. P. Hegarty, G. Huyet, J. G. McInerney, and K. D. Choquette, Phys. Rev. Lett. **82**, 1434 (1999).
[15] M. P. van Exter, A. K. Jansen van Doorn, and J. P. Woerdman, Phys. Rev. A **56**, 845 (1997).
[16] J. D. Jackson, *Classical Electrodynamics* (Wiley, New York, 1975), Chap. 8.
[17] J. Pollet, O. Méplan, and C. Gignoux, J. Phys. A **28**, 7282 (1995).
[18] J. V. Schwinger, in *Quantum Theory of Angular Momentum*, edited by L. C. Biederharn and H. Van Dam (Academic, New York, 1965).
[19] V. Bužek and T. Quang, J. Opt. Soc. Am. B **6**, 2447 (1989).
[20] L. A. Lugiato, C. Oldano, and L. M. Narducci, J. Opt. Soc. Am. B **5**, 879 (1988).
[21] R. Akis, D. K. Ferry, and J. P. Bird, Phys. Rev. Lett. **79**, 123 (1997).
[22] I. V. Zozoulenko and K. F. Berggren, Phys. Rev. B **56**, 6931 (1997).